0pt

August 27-31, 2023
FLORENCE - ITALY
ICWE 16
16th International Conference on Wind Engineering

LES-based multi-fidelity framework for wind loading

Mattia Fabrizio Ciarlatani[1], Themistoklis Vargiemezis[1], Catherine Gorlé[1]

[1]*Stanford University, Stanford, US, mattiafc@stanford.edu, tvarg@stanford.edu, gorle@stanford.edu*

SUMMARY:
This work investigates the use of a large-eddy simulation (LES) based multi-fidelity (MF) model for wind loading predictions on a high-rise building. The model aims at reducing the computational time required for wind loading predictions for the full wind rose. We combine data from a coarse LES, low fidelity (LF) model evaluated at a large number of wind directions with data from a fine LES, high fidelity (HF) model evaluated at a subset of those wind directions, and provide predictions for all wind directions with accuracy close to that of the HF model at a reduced cost. To do so, we train Neural Networks (NN) to learn the discrepancy between LF and HF at wind directions for which we have both LF and HF data, and then we use them to correct LF predictions for wind directions at which HF data is not available. We validate these neural network predictions against HF data and compare the results against a previously developed framework that employs Co-Kriging to perform the same task. The results show that the proposed multi-Fidelity framework provides accurate results in terms of mean, root-mean-square (rms), peak min, and peak max pressure coefficient (C_p) and outperforms Co-Kriging in terms of predictive capabilities.

Keywords: Multi-fidelity modeling, Neural networks, Wind loading predictions.

1. INTRODUCTION

Computational Fluid Dynamics (CFD) can play an important role in estimating wind loading on high-rise buildings. However, to enable its routine use for building design, a significant computational speed-up is required. To do so, we aim to combine data from cheap, low-fidelity (LF) large-eddy simulations (LES) with data from expensive, high-fidelity (HF) LES in a multi-fidelity (MF) framework to predict wind loading on the facade of a high-rise building for the full wind rose. In particular, we will combine LF data computed at 10 wind directions with HF data computed at 5 to provide wind loading predictions with accuracy close to the HF model at a fraction of its cost (i.e. 50% cost reduction).

2. CASE STUDY AND LES DATA SET

We consider the flow around a 1:50 scale rectangular plan high-rise building with an incoming neutral atmospheric boundary layer (ABL). The building model has a height, width, and breadth of respectively 2m, 0.3m, and 1m. Figure 1a shows the building schematic. The reader is referred to Lamberti et al., 2020 for more details on the model.

The Quantities of Interest (QoIs) for this work are the mean, rms, peak max, and peak mean

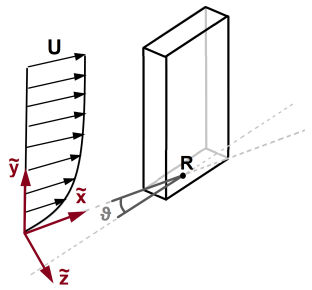

(a) High-rise building schematic.

(b) Taps distribution on the building surface.

Figure 1. High-rise building model and pressure taps distribution on its surface.

pressure coefficients on the building surface:

$$C_p^{mean} = \frac{\overline{p}}{\frac{1}{2}\rho U_H^2}; \quad C_p^{rms} = \frac{\overline{p'^2}}{\frac{1}{2}\rho U_H^2}; \quad C_p^{peak,max} = \frac{\widehat{p}}{\frac{1}{2}\rho U_H^2}; \quad C_p^{peak,min} = \frac{\breve{p}}{\frac{1}{2}\rho U_H^2}; \tag{1}$$

where p is the pressure, ρ is the standard air density, and U_H is the ABL velocity at roof height, which is $7.8 m/s$. The over-line $\overline{(.)}$ represents time-averaged quantities, the prime $(.)'$ represents temporal fluctuations, while $\widehat{(.)}$ and $\breve{(.)}$ indicate peak quantities computed using the extreme value analysis outlined in Cook and Mayne, 1980.

Our dataset consists of a low-fidelity and a high-fidelity set of LES simulations. The difference between the two sets of simulations is their mesh resolution: the control volumes used for the low-fidelity mesh are 2.3 times larger in each direction than the ones used for the high-fidelity mesh. Each LES setup is used to evaluate the wind loading on the building façade for 10 different wind directions in the $[0°;90°]$ interval. The time series of the pressure on the building surface from each LES is sampled at $\sim$ 1500 pressure taps. Figure 1b shows the pressure taps distribution on the building surface. The data is processed to construct adimensional, Galilean invariant features that will be used to train the neural network.

3. FRAMEWORK AND NEURAL NETWORK ARCHITECTURE

In this study, we combine data from LF simulations evaluated at all 10 wind directions with data from HF simulations evaluated at 5 of those wind directions to build the multi-fidelity model. We then investigate if the multi-fidelity model can accurately predict the HF model response at the 5 wind directions at which we withheld HF data when building the model. To do so, we train neural networks to learn the discrepancy $\Delta C_{p,i}$ between LF and HF data for every pressure coefficient at all locations of interest:

$$\Delta C_{p,i} = C_{p,i}^{HF} - C_{p,i}^{LF}; \tag{2}$$

where i denotes either the mean, rms, peak max, or peak min pressure coefficient at a specific location, HF denotes the HF model predictions, while LF denotes the LF model predictions. We train the neural network with features from LF and HF data from the 5 wind directions at which we have both HF and LF data using $\Delta C_{p,i}$ as labels. Then, we use features from LF data at the 5 wind directions at which we withheld HF to compute the HF-LF model discrepancy with the neural network model and we use it to correct the LF model response.

In this initial study, we adopt a multi-task neural network architecture that directly outputs all the QoIs. Figure 2 shows the neural network architecture. The first "shared" layers of neurons of the network are shared by the four tasks. This allows the network to gain some knowledge on shared traits among the tasks. After the last shared layer, the neural network branches out into multiple dedicated layers for each task, and each branch outputs the discrepancy described in equation (2). Finally, the discrepancy is used to correct the model response and predict the QoIs. We use ADAM to compute the neural network parameters update along with minibatch gradient descent. We define the loss L to be

$$L = \frac{RMSE_{NN}}{RMSE_{LES} + 1} \tag{3}$$

where $RMSE$ is the root-mean-squared error, NN denotes the neural network predictions, and LES denotes the LES predictions. This loss allows to account for the relative improvement provided by the Multi-fidelity framework with respect to LES results. To account for the non-uniform pressure tap distribution on the building surface, we define the $RMSE$ as

$$RMSE_i = \sqrt{\frac{\sum_{\mathbf{x},\theta} A(\mathbf{x},\theta)(C_p^i(\mathbf{x},\theta) - C_p^{HF}(\mathbf{x},\theta))^2}{\sum_{\mathbf{x},\theta} A(\mathbf{x},\theta)}}; \tag{4}$$

where i denotes either NN or LF, $\mathbf{x}$ represents the pressure tap location on the building surface, θ is the wind direction, and A is the tributary area of each pressure tap.

We tune the neural networks in terms of number of shared layers, number of individual layers, number of neurons for each layer, learning rate, and batch size. To tune the hyperparameters we use random grid search, and to reduce the parameter space we use the same architecture for each set of individual layers.

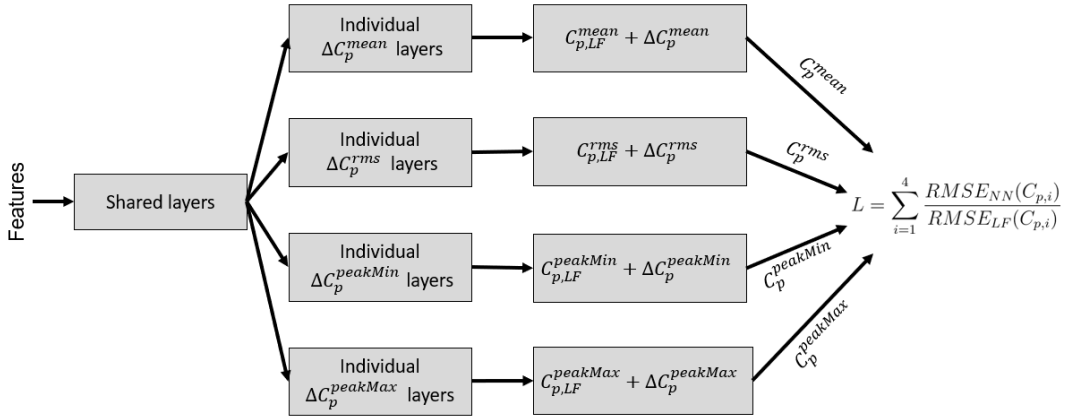

Figure 2. Neural network architecture. HF and LF features enter the layers shared by the four tasks, which eventually branch out into one individual layer for each task, each with the same number of layers and neuron per layer. The individual layers output the discrepancies, which are then used to predict the HF model response.

4. PRELIMINARY RESULTS

This section considers the case of an equispaced dataset: we use HF and LF data in $\{0°;20°;40°;60°;80°\}$ while we withheld HF data in $\{10°;30°;50°;70°;90°\}$. Table 1 compares the RMSE of the LF and

the NN model responses with respect to the HF responses. The results show that the NN consistently improves the LF model responses by reducing the LF model RMSE from 39% to 58%. Figure 3 shows a comparions of the low-fidelity, multi-fidelity, and high-fidelity model predictions for the rms C_p for a wind direction we did not use to train the neural network (i.e. 90°)

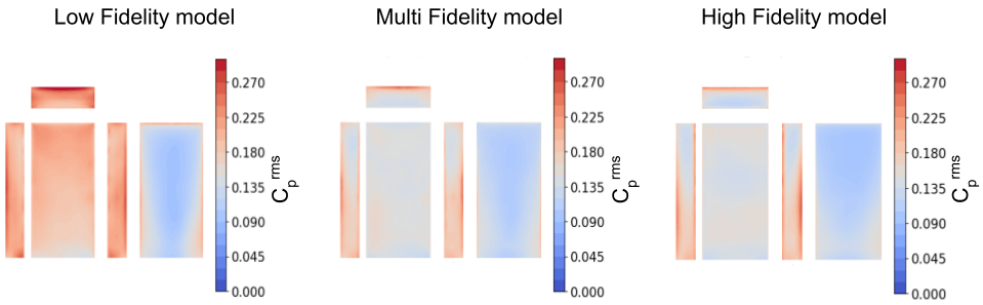

Figure 3. Comparison of the LF, MF, and HF model predictions for the rms C_p for the 90° wind direction.

To make a more insightful comparison, we can evaluate the percentage of the building surface over which the NN and the LF model predictions fall within a reasonable margin from the HF model predictions. These margins are defined as ± 0.1 for C_p^{mean}, ± 0.05 for C_p^{rms}, and ± 0.2 for both $C_p^{peak,min}$ and $C_p^{peak,max}$. To do so, we first compute the absolute error of the NN and the LF model at every point on the building surface, and then we use the points' tributary area to estimate the portion of the building surface over which the predictions fall within the aforementioned bounds. Table 2 shows the results of such a procedure. The table clearly shows that the NN significantly reduces the LF model error and yields acceptable results over most of the building surface.

Table 1. RMSE comparison between

	C_p^{mean}	C_p^{rms}	$C_p^{peak,min}$	$C_p^{peak,max}$
$RMSE_{NN}$	0.0394	0.0173	0.113	0.0512
$RMSE_{LF}$	0.0650	0.0371	0.195	0.121

Table 2. Percentage of the building area over which QoIs are predicted within reasonable bounds.

	C_p^{mean}	C_p^{rms}	$C_p^{peak,min}$	$C_p^{peak,max}$
Neural Network	97%	97%	92%	99%
Low-fidelity model	92%	82%	77%	91%

ACKNOWLEDGEMENTS

This material is based upon work supported by the NSF CAREER Award Number 1749610 and was developed with support from NSF grants 1053575 and 1548562. We would like to acknowledge high-performance computing support from Cheyenne (doi:10.5065/D6RX99HX) provided by NCAR's CISL, sponsored by NSF.

REFERENCES

Cook, N. and Mayne, J., 1980. A refined working approach to the assessment of wind loads for equivalent static design. Journal of Wind Engineering and Industrial Aerodynamics 6, 125–137.

Lamberti, G., Amerio, L., Pomaranzi, G., Zasso, A., and Gorlé, C., 2020. Comparison of high resolution pressure measurements on a high-rise building in a closed and open-section wind tunnel. Journal of Wind Engineering and Industrial Aerodynamics 204, 104247.